

Effect of Collagenase and Hyaluronidase on Free and Anomalous Diffusion in Multicellular Spheroids and Xenografts

LIVE EIKENES, INGUNN TUFTO, EDRUN A. SCHNELL,
ASTRID BJØRKØY and CATHARINA DE LANGE DAVIES

Department of Physics, Norwegian University of Science and Technology, 7491 Trondheim, Norway

Abstract. *Background: A critical step in the delivery of nanomedicines to tumour cells is transporting these particles through the extracellular matrix. Tumour-specific anticancer agents, such as encapsulated drugs, proteins, and genes, show low uptake in tumour tissue. It is not clear whether the collagen network or the glycosaminoglycan gel plays the most important role in limiting the interstitial transport of macromolecules. Therefore, we measured the effect of the collagen- and hyaluronan-degrading enzymes, collagenase and hyaluronidase, on interstitial diffusion. Materials and Methods: Human osteosarcomas were grown as multicellular spheroids and xenografts in dorsal skinfold window chambers. Diffusion of fluorescein isothiocyanate (FITC)-dextran molecules was measured by fluorescence recovery after photobleaching based on two-photon scanning laser excitation. Results: Collagenase, hyaluronidase, and relaxin increased the diffusion coefficient of the 2-MDa FITC-dextran in the spheroids, but 150-kDa FITC-dextran diffusion was not affected by the enzymatic treatment. In tumour tissue in vivo, collagenase and hyaluronidase increased the diffusion of the 150-kDa FITC-dextran. In xenografts, anomalous diffusion occurred, whereas only free diffusion was seen in spheroids. Conclusion: The results indicate that the collagen network has a greater impact on the interstitial diffusion of macromolecules in tumour tissue than the hyaluronan gel.*

Successful therapies based on novel nanomedicines, such as encapsulated drugs, proteins, or genes, require that the therapeutic agent reaches its target. A major barrier is having these macromolecules penetrate the extracellular matrix (ECM). This transport process is governed by diffusion and convection. Diffusion is the dominant mechanism of

interstitial transport for small solutes. Due to the elevated interstitial fluid pressure in solid tumours, the driving force for convection is lacking, and diffusion becomes the main transport mechanism for macromolecules, such as nanomedicines (1, 2). However, diffusion is a slow process for large molecules, resulting in a low and heterogeneous uptake in tumour tissue of anticancer agents such as monoclonal antibodies and liposomes (1, 3). When diffusion becomes the main transport mechanism, estimation of the diffusion coefficients of the therapeutic molecule is of clinical importance and may predict which macromolecules will be successfully delivered.

The ECM consists of a structural collagen network embedded in a gel of glycosaminoglycans (GAGs) and proteoglycans. However, it is not clear whether the collagen network or the GAG gel plays the most important role in limiting the interstitial transport of macromolecules. Macromolecular diffusion in tumours decreases with increasing collagen content (4, 5), and the collagen-degrading enzyme collagenase increases the diffusion rate of IgG in tumours (4, 6). On the other hand, hyaluronan, which is the predominant GAG, is positively correlated with the diffusion coefficient of IgG in tumours (5). In addition, the hyaluronan-degrading enzyme hyaluronidase increases the fraction of slowly diffusing IgG in tumours (6). When comparing the uptake of the osteosarcoma-associated antibody, TP-3, and liposomal doxorubicin after collagenase and hyaluronidase treatment, degrading the collagen network seemed to have a greater impact on the uptake of large molecules, such as IgG, whereas hyaluronidase favoured the uptake of small drugs, such as doxorubicin, administered in liposomes (7).

We previously found that hyaluronidase and collagenase increase convection by inducing transcapillary pressure gradients in human osteosarcoma xenografts (1, 8). The purpose of the present work was to compare the effect of hyaluronidase and collagenase on interstitial diffusion and to clarify if enhanced diffusion, in addition to convection, can improve tumour uptake of macromolecules. We also measured the effect of recombinant human relaxin on diffusion. Relaxin is a non-toxic hormone reported to both

Correspondence to: Catharina de Lange Davies, Department of Physics, Norwegian University of Science and Technology, Høgskoleringen 5, 7491 Trondheim, Norway. e-mail: catharina.davies@ntnu.no

Key Words: Interstitial diffusion, collagenase, hyaluronidase, two-photon excitation, FRAP.

stimulate collagenase production and down-regulate collagen production, and may be an alternative to collagenase treatment. Diffusion was measured both in human osteosarcomas that were grown as multicellular spheroids and in dorsal skinfold window chambers by fluorescence recovery after photobleaching (FRAP), based on two-photon scanning laser excitation. Dextran molecules of various sizes were used as the macromolecules. Diffusion in tissue may be a complex process that cannot be described by a free diffusion model (9, 10); thus, both anomalous and free diffusion models were compared.

Materials and Methods

Cell lines and multicellular spheroids. The human osteosarcoma cell line, OHS, was established at the Norwegian Radium Hospital from a patient with multiple skeletal manifestations of osteosarcoma (11). Multicellular spheroids were formed by the liquid overlay technique. Briefly, 2×10^6 cells were seeded in 80-cm² tissue culture flasks (Nunc, Tamro AS, Skårer, Norway) that were pre-coated with 1% agar to prevent cell attachment. Cells were grown in 25 ml growth medium (RPMI-1640) supplemented with 10% foetal bovine serum, 100 units/ml penicillin/streptomycin, and 1 mM L-glutamine (all from Sigma, St. Louis, MO, USA). The spheroids were grown at 37°C and 5% CO₂. Half of the medium was changed twice a week. Spheroids were harvested after 5-6 days, when their diameters had reached 150-250 µm. The growth curve for the spheroids has been reported previously and corresponded well with the Gompertz curve. The spheroids had no histologically visible necrosis (12).

Tumours grown in a dorsal skinfold window chamber. The OHS cells were grown as xenografts in skinfold window chambers on the back of female athymic BALB/c *nu/nu* mice (10-16 weeks, 24-27 g; Taconic M&B, Ry, Denmark), and the chambers were implanted as described previously (7). Briefly, the mice were anaesthetised by *i.p.* injection of 12 ml/kg body weight of haldol/fentanyl/ midazolam/sterile water (2:3:3:4) (Janssen-Cilag AS, Oslo, Norway; Hameln Pharmaceuticals, Hameln, Germany; Alparma AS, Oslo, Norway). An extended double layer of skin was sandwiched between two symmetrical titanium frames, and a 15-mm circular area of one of the layers of skin was completely removed. The remaining layers were covered with a glass coverslip. Twenty-four hours after the implantation, 1.5×10^6 OHS cells were placed into the centre of the chamber. The tumours were grown for 14-16 days. The animals tolerated the chamber well and showed no signs of discomfort. The animals were kept under pathogen-free conditions at a constant temperature of 24-26°C and 30-50% humidity and were allowed food and water *ad libitum*. All animal experiments were carried out with Ethical Committee approval. The ethical guidelines that were followed meet the standard required by the UKCCCR guidelines.

Enzymes and fluorescent tracers. The ECM degrading enzymes, collagenase (Clostridiopeptidase A; Sigma) and bovine testicular hyaluronidase (Neopermease®; Sandoz-Novartis, kindly provided by Professor G Baumgartner (applied to spheroids) or Hylase Dessau; Riemsers Arzneimittel AG, Greifswald-Insel Riems, Germany (applied to tumours)), were used to modify the collagen and

hyaluronan content and structure in the spheroids and in the tumour tissue. Neopermease® was provided at a higher concentration than Hylase Dessau and, therefore, was used in the dose response study in spheroids. In addition, recombinant human relaxin (rhRlx; BAS Medical, San Mateo, CA, USA) was used to modify collagen in the spheroids by stimulating collagenase expression and down-regulating collagen synthesis and secretion (13).

The spheroids were either preincubated with the enzymes for 1 h before removing the medium containing enzymes and adding fresh medium with 2-MDa FITC-dextran (1 mg/ml; Sigma) for 18 h, or the enzymes and 2-MDa FITC-dextran or 150-kDa FITC-dextran (1 mg/ml; Sigma) were incubated together for 18 h. The incubation took place on a roller at 37°C. To study the dose response of the enzymatic treatment on diffusion, the collagenase doses used were 1 mg/ml, 5 mg/ml and 10 mg/ml. The high hyaluronidase dose of 150,000 units/ml was used for the 1 h incubation and lower doses of 300, 3,000, and 30,000 units/ml for the 18 h incubation. Spheroids were treated either with 1.4 mg/ml of recombinant human relaxin for 1 h, 18 h, and 2 days, or with a 0.5 mg/ml dose for 4 days. After incubation, the spheroids were transferred to a specially designed imaging glass chamber together with the fluorescent macromolecular solution for diffusion measurements.

Diffusion of 150-kDa FITC-dextran in tumour tissue in the dorsal window chambers was measured 24 h and 48 h after enzymatic treatment with either 100 µl 1 mg/ml collagenase or 100 µl 1500 units hyaluronidase injected *i.v.* in the tail vein. The doses of collagenase and hyaluronidase used in this study were the same doses that reduced the interstitial fluid pressure to the largest extent (1, 8). 150-kDa FITC-dextran (200 µl 30 mg/ml) was injected 1 h after the enzymatic treatment and diffusion measured the following day. An additional injection of 150-kDa FITC-dextran was given after the 24 h diffusion measurement and diffusion measured once more the following day.

The tumour blood vessels were visualised by *i.v.* injection of 200 µl 10 mg/ml 2-MDa tetramethylrhodamine (TMR)-dextran (Molecular Probes, Eugene, OR, USA).

Imaging and diffusion measured by fluorescence recovery after photobleaching (FRAP). The distribution of FITC-dextran molecules and blood vessels were imaged using confocal laser scanning microscopy (LSM 510; Carl Zeiss, Jena, Germany). Three-dimensional diffusion was measured based on FRAP using two-photon laser excitation together with scanning microscopy, as described previously (14). A C-Apochromat 40x/1.2 W Corr. objective was used for measurements in spheroids, and a C-Achroplan 40x/0.8 W Corr. objective with a long working distance was used for measurements in tumours growing in chambers. FITC was excited at 780 nm by mode locked Ti:sapphire laser (Mira Model 900-F; Coherent, Inc., Laser Group, Santa Clara, CA, USA), which was pumped by a solid state laser (Verdi V-2/V-5; Coherent, Inc., Laser Group) at 532 nm. The Ti:sapphire laser produces ~200 fs pulses at a repetition rate of 76 MHz; at a 780 nm excitation, the typical output power was 850 mW at the exit of the Ti:sapphire crystal and approximately 30-50 mW at the objectives. A 543 nm HeNe laser was used to excite the TMR-dextran.

The FRAP experiments started with 10 image scans of the region of interest (ROI), followed by a bleach pulse of approximately 150 ms. The bleached ROI had a radius of 3.6 µm and 0.9 µm in spheroids and tumour tissue, respectively. In tumour tissue, a zooming factor to reduce the pixel size from 0.45 µm to 0.11 µm was necessary in order

to obtain sufficient fluorescence intensity per pixel when using the Achroplan objective. A series of 190 images were subsequently collected at the highest possible acquisition rate of 25.1 ms (duration of the acquisition of the ROI-image plus the shortest possible time between each acquisition). During imaging, the laser power was attenuated to approximately 5% of the 100% bleach intensity. In spheroids, the measurements were performed approximately 30 μm inside the spheroids.

A prerequisite for correct estimation of the diffusion coefficient using FRAP is that no diffusion takes place during bleaching. In a previous study, we have shown that diffusion of macromolecules occurred during bleaching in solution, but not in the tumour tissue, when using the bleaching time indicated in the present work (14).

Mathematical modelling of the diffusion coefficient. We have previously developed a model to determine the diffusion coefficient from the fluorescence recovery curves after two-photon bleaching with a scanning laser microscope (14). In the case of single freely diffusing species in three dimensions, assuming a Gaussian bleaching profile, the time-dependent fluorescence signal after two-photon excitation and two-photon bleaching is given by:

$$\frac{F(t)}{F_\infty} = 1 - \frac{F_\infty - F(0)}{F_0 - F(0)} \left(1 - \sum_{n=0}^{\infty} \frac{(-\beta)^n}{n!} \frac{1}{\left(1 + n \left(1 + \frac{16Dt}{\omega_r^2}\right)\right)} \sqrt{\frac{1}{1 + n \left(1 + \frac{16Dt}{\omega_z^2}\right)}} \right) \quad (\text{Eqtn 1})$$

where D is the diffusion coefficient of the fluorophore, β is the bleach depth parameter, and ω_r and ω_z are the radial and axial $1/e^2$ radius of the bleached area, respectively. The bleach radii were determined experimentally for the two objectives and zooming factors (14). The model also includes the mobile fraction:

$$R = \frac{F_\infty - F(0)}{F_0 - F(0)} \quad (\text{Eqtn 2})$$

where F_0 is the mean intensity of the first 10 images before bleaching, $F(0)$ is the intensity at time=0 after bleaching, and F_∞ the intensity of the bleached spot at an infinite time after bleaching.

In tissue, the diffusion coefficient may vary with time, and the mean square displacement obeys a power law in time

$$\langle r^2 \rangle = 4D(t)t = 4\Gamma t^\alpha \quad (10),$$

where α is the anomalous diffusion parameter that determines if the diffusive motion is retarded by the microenvironment (subdiffusive, $\alpha < 1$) or if there are other transport processes in addition to diffusion that contribute to the molecular transport (superdiffusive, $\alpha > 1$). For $\alpha = 1$, the equation is reduced to the model for free diffusion. Thus, the anomalous diffusion model was also fitted to the experimental recovery curve:

$$\frac{F(t)}{F_\infty} = 1 - \frac{F_\infty - F(0)}{F_0 - F(0)} \left(1 - \sum_{n=0}^{\infty} \frac{(-\beta)^n}{n!} \frac{1}{\left(1 + n \left(1 + \frac{16(Dt)^\alpha}{\omega_r^2}\right)\right)} \sqrt{\frac{1}{1 + n \left(1 + \frac{16(Dt)^\alpha}{\omega_z^2}\right)}} \right) \quad (\text{Eqtn 3})$$

where the terms, Dt , in the model for free diffusion are replaced with terms of the form $(Dt)^\alpha$ (15).

Non-free diffusion may be either anomalous or multi-component. The anomalous diffusion model was therefore compared to a two-component model:

$$\frac{F(t)}{F_\infty} = 1 - \frac{F_\infty - F(0)}{F_0 - F(0)} N_1 \frac{F_\infty - F(0)}{F_0 - F(0)} \left(\sum_{n=0}^{\infty} \frac{(-\beta)^n}{n!} \frac{1}{\left(1 + n \left(1 + \frac{16Dt}{\omega_r^2}\right)\right)} \sqrt{\frac{1}{1 + n \left(1 + \frac{16Dt}{\omega_z^2}\right)}} \right) + N_2 \frac{F_\infty - F(0)}{F_0 - F(0)} \left(\sum_{n=0}^{\infty} \frac{(-\beta)^n}{n!} \frac{1}{\left(1 + n \left(1 + \frac{16Dt}{\omega_r^2}\right)\right)} \sqrt{\frac{1}{1 + n \left(1 + \frac{16Dt}{\omega_z^2}\right)}} \right) \quad (\text{Eqtn 4})$$

where N_1 and N_2 are the relative fractions of the two species.

Equations 1, 3, and 4 were fitted to the experimental recovery curves to estimate the diffusion coefficients, the bleaching parameters, and the anomalous diffusion parameters using the Matlab 7.0 lsqcurvefit function for solving nonlinear least square problems (MathWorks Inc, Natick, MA, USA).

Measurements of collagen and hyaluronan content in spheroids and tumours. The levels of collagen and hyaluronan in subcutaneous tumours have been reported previously (16). In the present work, the ECM constituents were measured in spheroids as described for tumours (16). Briefly, the spheroids were homogenised and placed in a digestion buffer for 18 h at 60°C. The amount of collagen was determined by measuring hydroxyproline according to Woessner (17) and by assuming 6.94 μg collagen per μg hydroxyproline (18). The total amount of GAG was determined by the reaction of uronic acid with carbazole, as described by Bitter and Muir (19). Sulphated GAG (s-GAG) was measured using the Blyscan proteoglycan and s-GAG assay (Biocolor Ltd, Belfast, Ireland), which is based on the specific binding of the cationic dye, 1,9 dimethylmethylene blue (20). The content of hyaluronan was estimated as the difference between total GAG and s-GAG, both expressed equivalent to uronic acid.

Statistical analysis. Two-sample two-tailed Student's t -tests assuming non-equal variances were applied to the Gaussian-distributed data to compare population means (Minitab; Minitab Inc., State College, PA, USA). All statistical analyses were performed using the significance criterion of $p \leq 0.05$.

The quality of the fit between the experimental recovery curve and the mathematical model was determined by the least squares regression method and given by the squared coefficient of multiple correlation (R^2) and the residual sum of squares (RSS). The differences in R^2 and RSS for the free and anomalous model relative to the free model were calculated.

Results

FRAP measurements in spheroids and tumours. Multiphoton FRAP measurements were performed in the ECM in OHS spheroids and OHS xenografts grown in dorsal window chambers. In spheroids, both sized macromolecules (150-kDa and 2-MDa FITC-dextran) were homogeneously distributed throughout the ECM (Figure 1A). In the xenografts, however, the macromolecules (150-kDa FITC-dextran) were heterogeneously distributed throughout the

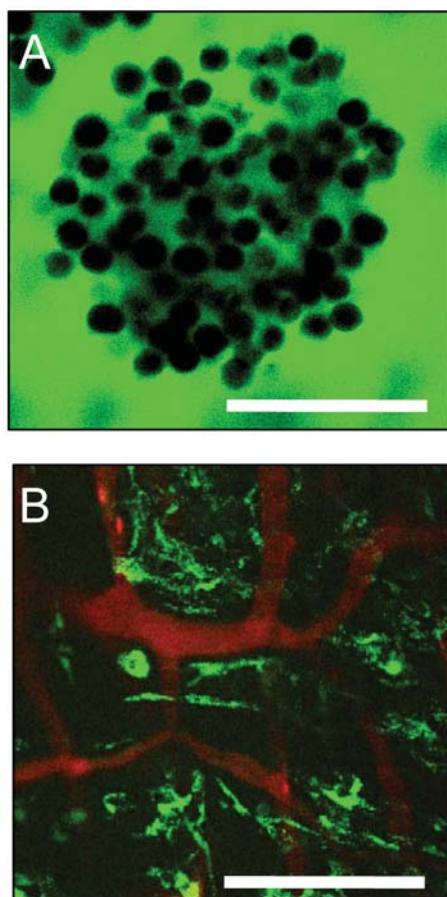


Figure 1. A: A multicellular OHS spheroid incubated with 150-kDa FITC-dextran (green). Bar=100 μ m. B: Localisation of 150-kDa FITC-dextran (green) and the tumour vasculature injected with 2-MDa TMR-dextran (red) in a representative OHS tumour grown in a dorsal window chamber. Bar=100 μ m.

tumour tissue and were primarily located in clusters around tumour cells adjacent to blood vessels (Figure 1B).

The fluorescence recovery curves for 150-kDa FITC-conjugated dextrans in PBS, spheroids, and tumour tissue in dorsal chambers are compared in Figure 2. The lines represent the free diffusion model (Equation 1) fitted to the experimental recovery data, resulting in average diffusion coefficients of $19.0 \times 10^{-8} \text{ cm}^2/\text{s}$ (PBS), $15.3 \times 10^{-8} \text{ cm}^2/\text{s}$ (spheroids), and $2.4 \times 10^{-8} \text{ cm}^2/\text{s}$ (tumours). The diffusion coefficient of the dextran molecule measured in solution corresponded well with previously published experimental values (21). The diffusion coefficient decreased with the complexity of the system from solution to tissue (Figure 2) and also decreased with increasing molecular weight in spheroids (Figure 3A-C). The diffusion coefficient of 150-kDa FITC-dextrans decreased by approximately 20 and 90% in spheroids and tumour tissue, respectively, compared to solution.

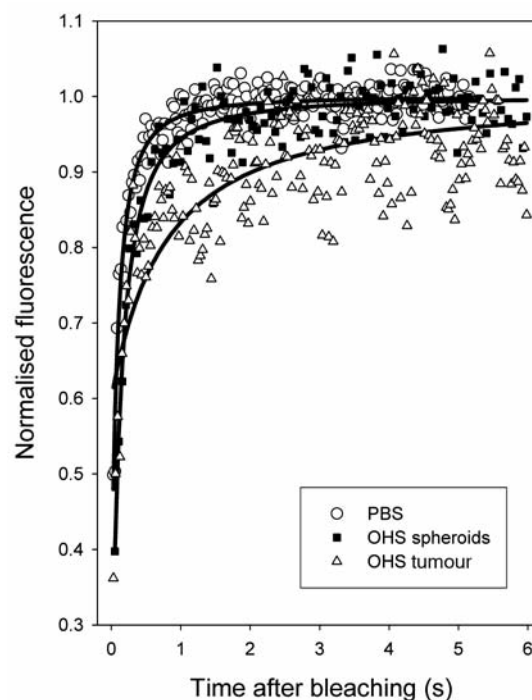


Figure 2. Normalised fluorescence recovery curves after photobleaching of 150-kDa FITC-dextrans in PBS (\circ), OHS spheroids (\bullet), and OHS tumours grown in dorsal window chambers (\triangle). The lines represent the model assuming free diffusion of the normalised fluorescence after photobleaching fitted to the experimental data, resulting in diffusion coefficients of $19.0 \times 10^{-8} \text{ cm}^2/\text{s}$ (PBS), $15.3 \times 10^{-8} \text{ cm}^2/\text{s}$ (OHS spheroids), and $2.4 \times 10^{-8} \text{ cm}^2/\text{s}$ (OHS tumours).

The mobile fraction of the macromolecules was also calculated from the recovery curves. The spheroids had a low fraction of bound macromolecules, about 2-4%, indicating that the macromolecules diffuse freely in the spheroids. However, the bound fraction of the macromolecules in the tumour tissue was high, ranging from 20-60% depending on the site of measurement; in some locations, no recovery was seen at all.

The high degree of immobilised molecules indicates an anomalous subdiffusion (10); therefore, the experimental recovery curve was fitted to the anomalous model. Anomalous diffusion was found in the tumour tissue (see below), but not in the spheroids, where the anomalous diffusion parameter α varied from 0.96 to 1.08, the same value as that reported for free diffusion (10).

Effect of collagenase, hyaluronidase, and relaxin on macromolecular diffusion in spheroids. Collagenase induced a dose-dependent increase in the diffusion coefficient of the 2-MDa FITC-dextrans when spheroids were incubated for 1 h, and the diffusion coefficient increased by 20% and 70% after 5 mg/ml and 10 mg/ml collagenase, respectively (Figure 3A).

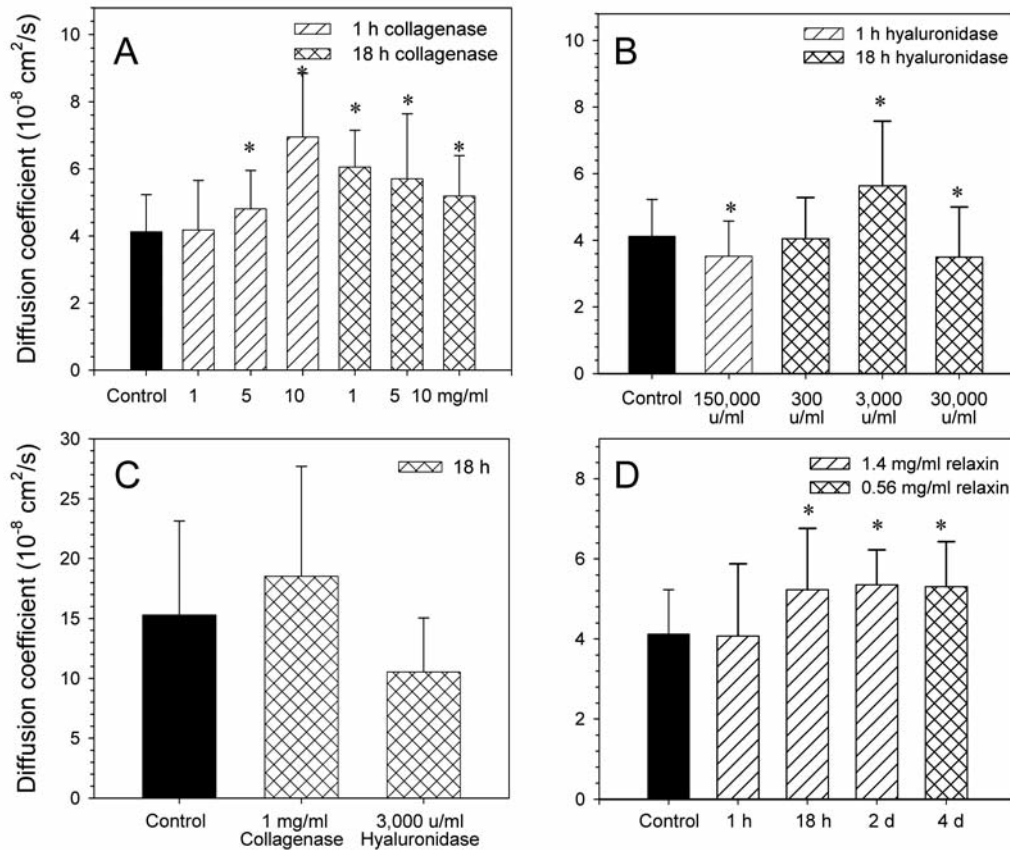


Figure 3. Diffusion coefficients of 2-MDa FITC-dextran in OHS spheroids treated with PBS (control), 1, 5, and 10 mg/ml collagenase for either 1 or 18 h (A); PBS (control), 150,000 units/ml hyaluronidase for 1 h or 300, 3,000 or 30,000 units/ml hyaluronidase for 18 h (B); Diffusion coefficients of 150-kDa FITC-dextran in OHS spheroids treated with PBS (control), 1 mg/ml collagenase and 3,000 units/ml hyaluronidase for 18 h (C); PBS (control), 1.4 mg/ml recombinant human relaxin for 1 h, 18 h, or 2 days or 0.56 mg/ml for 4 days (D). The diffusion coefficients are the mean of 20-40 measurements in A and B, 15-40 measurements in C, and 10-30 measurements in D. Bars indicate S.D., and * indicates data significantly different from untreated controls.

Incubation with 1 mg/ml collagenase for 1 h did not induce any significant change in the diffusion coefficient, while incubation with 50 mg/ml collagenase for 1 h totally degraded the spheroids (data not shown). Increasing the incubation time to 18 h increased the diffusion coefficient further for the two lowest doses. However, the diffusion coefficient decreased with increasing dose (Figure 3A).

Hyaluronidase exposure for 1 h did not increase the diffusion of 2-MDa FITC-dextran in spheroids. A dose of 3,000 units/ml had no effect (data not shown), whereas the higher dose of 150,000 units/ml reduced the diffusion coefficient significantly (15%) (Figure 3B). Hyaluronidase exposure for 18 h affected diffusion in a non-linear manner (Figure 3B). Only incubation with 3,000 units/ml hyaluronidase increased the diffusion coefficient (40%). Lower doses (300 units/ml) had no effect on diffusion, and the higher dose (30,000 units/ml) induced a significant reduction in the diffusion coefficients (15%).

The diffusion coefficient of the 150-kDa FITC-dextran was also measured in the spheroids, and no significant effect was observed after treatment with 1 mg/ml collagenase or 3,000 units/ml hyaluronidase for 18 h (Figure 3C). These two doses induced the highest increase in the diffusion coefficient of 2-MDa FITC-dextran.

Recombinant human relaxin significantly increased the diffusion coefficient of the 2-MDa FITC-dextran when given for a longer time period (Figure 3D). Incubation with 1.4 mg/ml relaxin for 18 h and 2 days or with 0.56 mg/ml relaxin for 4 days each increased the diffusion coefficient to the same extent (30%). Thus, increasing the exposure time from 1 to 2 days did not induce a further increase in the diffusion coefficient. A 1 h exposure did not induce any change in the diffusion coefficient.

Effect of collagenase and hyaluronidase on macromolecular diffusion in tumour tissue. Both collagenase and hyaluronidase increased the diffusion

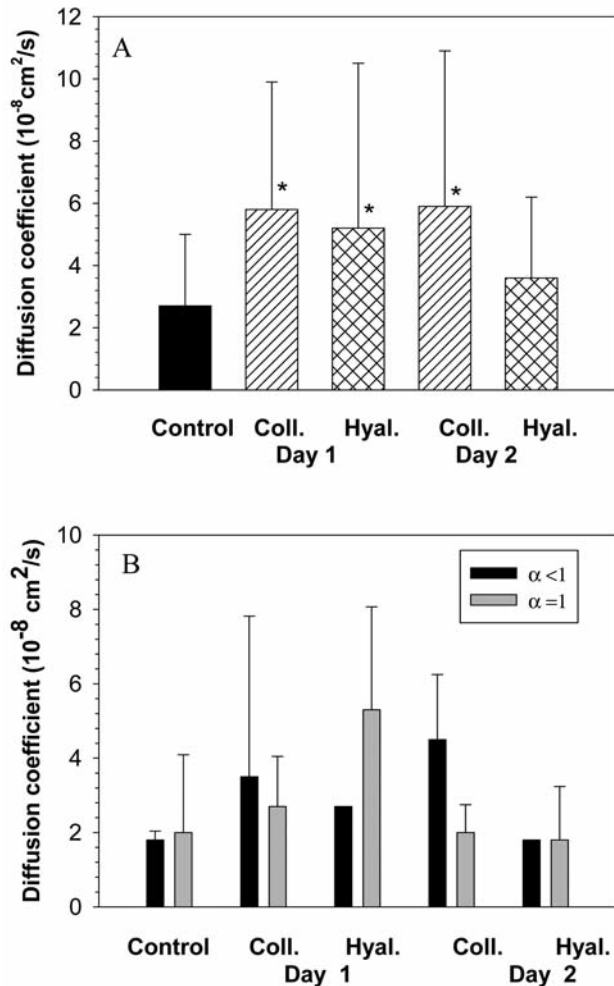


Figure 4. Diffusion coefficients of 150-kDa FITC-dextran in OHS tumours grown in dorsal window chambers in control tumours ($n=5$ tumours, 3-4 measurements per tumour) and in tumours treated with either 1 mg/ml collagenase ($n=4$ tumours, 29 measurements on day 1; 14 measurements on day 2) or 3,000 units/ml hyaluronidase ($n=4$ tumours, 14 measurements on day 1; 15 measurements on day 2): A, using a model of free diffusion; B, using a model for anomalous diffusion. The diffusion coefficients in each group are divided into two populations: $\alpha < 1$ (subdiffusion) and $\alpha = 1$ (free diffusion). Bars indicate S.D., and * indicates data significantly different from untreated controls.

coefficient of the 150-kDa FITC-dextran in the tumours grown in dorsal chambers.

When calculating the diffusion coefficient using the model assuming free diffusion, both collagenase and hyaluronidase increased the diffusion approximately two-fold, after one day of treatment (Figure 4A). Two days after treatment, however, the diffusion coefficient enhancement was maintained in the collagenase-treated tumours while the diffusion coefficient in the hyaluronidase-treated tumours was not significantly different from that of the control.

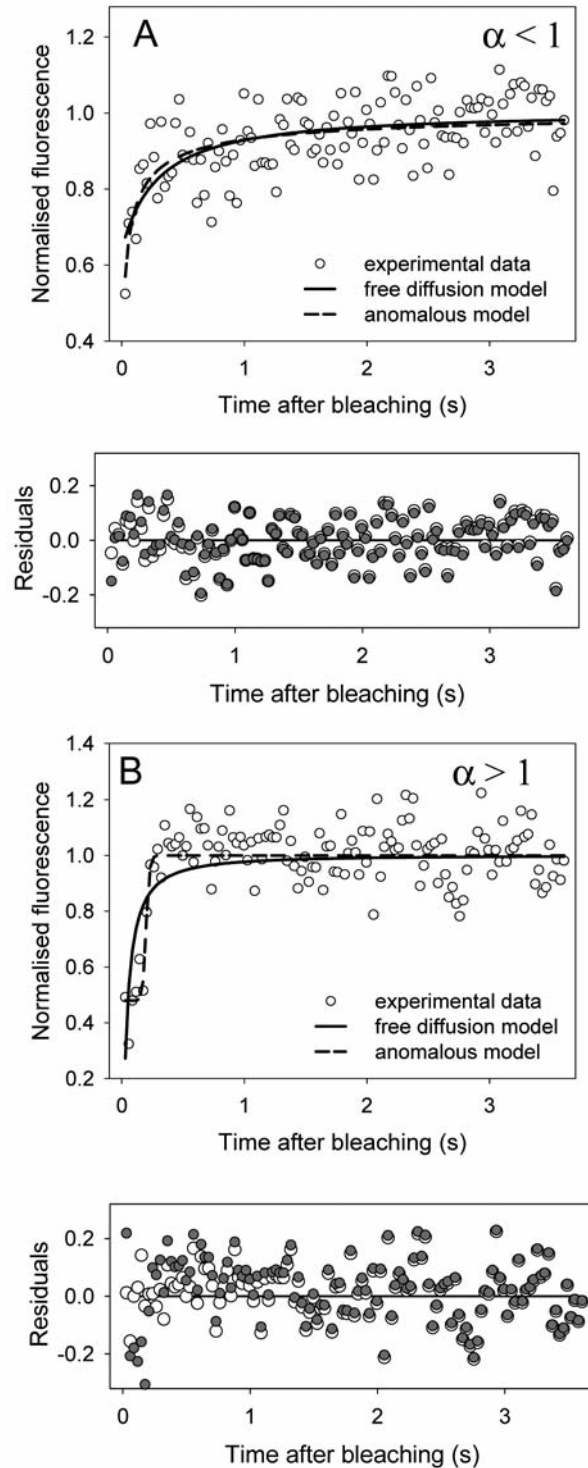


Figure 5. Normalised fluorescence recovery curves after photobleaching of 150-kDa FITC-dextran in OHS tumours grown in dorsal window chambers. The lines represent the free diffusion model (solid line) and the anomalous diffusion model (dashed line) of the normalised fluorescence after photobleaching fitted to the recovery data for $\alpha < 1$ (A) and $\alpha > 1$ (B). Corresponding residuals for the two fits are shown (closed and open symbols represent free and anomalous diffusion data, respectively).

The free diffusion model was then compared to the anomalous diffusion model. The anomalous diffusion model demonstrated a better quality of fit (Figure 5A). The R^2 parameter was always higher, and the RSS was lower for the anomalous model compared to the free diffusion model. When calculating the diffusion coefficient using the anomalous model, the diffusion coefficients could be grouped into three different categories: subdiffusion ($\alpha < 1$), free diffusion ($\alpha = 1$), and superdiffusion ($\alpha > 1$), depending on the location of the measurements.

Collagenase may have a greater impact on the diffusion coefficient in regions of the tumours where subdiffusion occurred compared to regions with free diffusion (Figure 4B), especially two days after the treatment when the diffusion coefficient was two-fold higher in the regions of subdiffusion compared to regions of free diffusion. Hyaluronidase, on the other hand, induced lower diffusion in the regions of subdiffusion compared to free diffusion. However, the number of measurements in the two categories of diffusion is low and there is no statistical difference between the two categories. In hyaluronidase-treated tumours, subdiffusion was observed only at one location. In cases where superdiffusion gave the best fit, the experimental data in the initial part of the recovery curve were oscillating, not increasing with time, and the mathematical fit showed an initial lag and a subsequently step curve (Figure 5B). Thus, the results indicating $\alpha > 1$ may not be due to enhanced transport but rather may reflect a poor model. Diffusion coefficients obtained when $\alpha > 1$ are therefore not included in Figure 4.

Fitting the experimental recovery curves to a two-component model resulted in one dominating population with $N_f = 0.9$ -1.0 and a diffusion coefficient somewhat larger than the anomalous diffusion coefficient. The diffusion coefficient of the other population was approximately 10-fold less. The quality of fit given by R^2 and RSS was, however, poorer than that for the anomalous model. In addition, the parameter dependencies of regression were close to 1.0, indicating that the equation was overparameterised.

Collagen and hyaluronan content in OHS spheroids and OHS tumours. The amounts of collagen and hyaluronan were measured in OHS spheroids. In subcutaneous OHS xenografts, the ECM constituents have been measured previously and are compared with these in spheroids in Table I (16). The OHS spheroids had a collagen and hyaluronan content of approximately one-third and 1.7 those of the subcutaneous tumours, respectively.

Discussion

The present work demonstrates that both collagenase and hyaluronidase can increase the diffusion of macromolecules in tumour tissue, which may partly explain the increased

Table I. Content of collagen, total GAG, s-GAG and hyaluronan in spheroids and tumour tissue growing subcutaneously. GAG, s-GAG and hyaluronan were measured equivalent to uronic acid (UA) per mg wet tissue.

Tissue	Collagen ($\mu\text{g}/\text{mg}$)	Tot GAG ($\mu\text{g UA}$ eqv/mg)	s-GAG ($\mu\text{g UA}$ eqv/mg)	Hyaluronan ($\mu\text{g UA}$ eqv/mg)
OHS spheroids	0.47 \pm 0.25	1.38 \pm 0.41	0.18 \pm 0.13	1.20 \pm 0.41
OHS xenografts	1.57 \pm 0.11	1.19 \pm 0.03	0.44 \pm 0.02	0.71 \pm 0.04

uptake of therapeutic molecules reported previously (1, 8). The results indicate that collagenase has a greater impact on the diffusion of macromolecules compared to hyaluronidase. Thus, degradation of the structural network of collagen is more important than the degradation of the hydrophilic gel of GAG and hyaluronan when attempting to increase the macromolecular diffusion coefficient.

However, in multicellular spheroids, the enhanced diffusion occurred only for larger macromolecules, such as 2-MDa dextrans, whereas enzymatic degradation of the ECM had no impact on diffusion of 150-kDa dextran. This indicates that the ECM of the spheroids is not a severe barrier for diffusion of the 150-kDa dextran, in accordance with the small difference in diffusion coefficient between 150-kDa dextrans in solution and spheroids. In tumour tissue, on the other hand, the diffusion coefficient of 150-kDa dextran was substantially reduced compared to solution, and the enzymatic treatment improved the diffusion.

Enzyme doses and incubation times are important to achieve optimal enhancement of diffusion of 150-kDa dextran in tumours and 2-MDa dextran in spheroids, and the kinetics were different for collagenase and hyaluronidase. After collagenase administration in mice, the increase in the diffusion coefficient was maintained for two days, whereas the diffusion was reduced to the same level as in control mice two days after hyaluronidase treatment. This effect may be due to differences in the half-lives of the two enzymes. In spheroids, a short incubation (1 h) with collagenase demonstrated a dose-dependent increase in diffusion of 2-MDa dextrans. Increasing the incubation time to 18 h resulted in a decrease in the diffusion coefficient with increasing doses. Thus, high doses of collagenase combined with long exposure times may severely degrade the collagen network, impeding diffusion. The severe degradation of the structural network may also induce a collapse of the hydrophilic GAG gel, thereby limiting further macromolecular diffusion. The resynthesis of collagen will repress the efficacy of collagenase, and a negative feedback regulation of collagen synthesis may increase the production of collagen with increasing degradation.

To improve diffusion by hyaluronidase, a long incubation period was needed, and hyaluronidase only increased the diffusion within a small dose interval. This type of dose-window has also been demonstrated for the effect of hyaluronidase on interstitial fluid pressure (8), and when measuring the ability to penetrate the epithelial luminal glycocalyx (22). Together, these results indicate that hyaluronan has a dual role in transport through the ECM. Hyaluronan polymerises into cage-like structures of approximately 15 nm in diameter, partitioning the interstitial space into aqueous and viscous compartments (23). At high concentrations, hyaluronan may serve as a viscous barrier to tracers but may simultaneously permit passage in the water-filled spaces. High doses of hyaluronidase may collapse these water-swelling cage structures of hyaluronan and induce crossbinding of the ECM fragments. This crossbinding would make the ECM more viscous and less permeable, thereby reducing the diffusion coefficient. The dose of hyaluronidase therefore seems to be of critical importance when modulating the ECM and may dictate the therapeutic outcome when given, for example, as an adjuvant to chemotherapy.

Consistent with our results, collagenase increased the diffusion of IgG in tumour tissue (4). In a study revealing both a fast and a slow component of diffusion in tumour tissue, collagenase increased the proportion of the fast-diffusing IgG (6). Hyaluronidase is reported to increase the proportion of slow-diffusing IgG in tumour tissue (6) and decrease the diffusion of albumin in normal tissue (24, 25). These contradictory results are in agreement with the dual effect of hyaluronidase observed in spheroids and support the idea that the effect of hyaluronidase is highly dependent on the dose and duration of exposure. The complexity of the tissue also seems to be of importance, as both collagenase and hyaluronidase had a greater impact on interstitial diffusion in tumour tissue *in vivo* than in spheroids *in vitro*. This result is probably due to the more complex ECM produced by the host stromal cells (5) and the greater level of collagen in xenografts compared to spheroids.

To establish whether the diffusion in spheroids and tumour tissue was free or restricted, the diffusion coefficients were calculated using both an anomalous and a two-component diffusion model. Based on the quality of fit and the low fraction of the second species in the two-component model (less than 10%), anomalous diffusion is more likely than two-component diffusion. Anomalous diffusion was found in tumour tissue but not in spheroids. In the tumours grown in dorsal window chambers, both subdiffusion and free diffusion were observed, depending on the location in the tissue. The anomalous subdiffusion is probably due to steric exclusion and the tortuosity of pathways arising from several factors, including collisions with obstacles such as proteins and cells, spatially varying hydrodynamics, and binding and noncovalent interactions (26). Transport by mechanisms other than

diffusion (superdiffusion) may be due to the directed transport of molecules and inhomogeneous fluid convection in tumour tissue (27). However, these factors are probably not the reason for obtaining the anomalous parameter $\alpha > 1$, but rather the oscillating initial portion of the recovery curve causing an initial lag and subsequently a step increase in the fit.

When estimating the diffusion coefficient using the anomalous model, collagenase may have a greater impact on the diffusion coefficient in regions of the tumours where subdiffusion occurred, compared to regions with free diffusion. Therefore, we speculate that collagenase reduces binding and noncovalent interactions and reduces the number of obstacles for the macromolecules. Hyaluronidase, on the other hand, did not influence subdiffusion to the same extent, indicating that the GAG gel had little impact on subdiffusion. Subdiffusion was only observed in one location in the hyaluronidase-treated tumours.

Enhanced diffusion after modifying collagen production was also demonstrated by the hormone relaxin. Relaxin increased the diffusion of the 2-MDa FITC-dextran in the spheroids, which is consistent with another study (28). However, increasing the dose or the incubation time did not increase the diffusion coefficient further. A previous study showed that a minimum of 18 h of relaxin exposure was necessary to detect an enhancement in procollagenase secretion (13). Others have shown that the equilibrium level of collagen is maintained after relaxin treatment, but that the collagen structure becomes more porous and therefore presents a weaker diffusive hindrance (28). Relaxin probably acts more slowly than collagenase and is not as efficient as direct enzymatic treatment. However, relaxin is a hormone that occurs naturally in the body and may be less damaging to healthy tissue and may not have the same metastatic and invasive properties as collagenase (29, 30). The invasive properties of relaxin are not clear, as short-term exposure *in vitro* seems to enhance invasiveness (31), whereas long-term exposure reduces it (32).

In previous studies, collagenase and hyaluronidase were found to increase the uptake of two therapeutic agents, liposomal doxorubicin (Caelyx™) and osteosarcoma-associated antibody (TP-3), in human osteosarcoma xenografts (1, 8, 33). The enhanced uptake of therapeutic molecules may be caused by both increased interstitial diffusion and the induction of a transcapillary pressure gradient. We previously found that both collagenase and hyaluronidase can reduce interstitial fluid pressure and can induce a transcapillary pressure gradient (1, 8). Various treatments have demonstrated a reduction in the interstitial fluid pressure, but to our knowledge, collagenase and hyaluronidase are the only treatments that have been studied with respect to both transport mechanisms: convection measuring the interstitial fluid pressure and the microvascular pressure, as well as diffusion. An enhanced transcapillary pressure gradient is

necessary for transcapillary transport, whereas the increased interstitial diffusion facilitates the penetration further into the ECM. Thus, enzymatic degradation of tumour tissue in combination with macromolecular anticancer therapy may improve the therapeutic outcome by improving both the transcapillary and interstitial transport.

Acknowledgements

We thank Kristin Sæterbø for growing cells *in vitro* and Baukje Kuitert and Christine Stanseberg for measuring collagen and hyaluronan content, respectively, in spheroids. We would also like to thank Professor G Baumgartner for supplying us with hyaluronidase (Neopermease®, Sandoz-Novartis), Riemser Arzneimittel AG (Greifswald-Insel Riems, Germany) for supplying us with Hylase Dessau, and BAS Medical for supplying us with recombinant human relaxin (rhRlx, BAS Medical, San Mateo, CA, U.S.A.). This work was supported by the Norwegian Cancer Society.

References

- Eikenes L, Bruland ØS, Brekken C and Davies CdeL: Collagenase increases the transcapillary pressure gradient and improves the uptake and distribution of monoclonal antibodies in human osteosarcoma xenografts. *Cancer Res* 64: 4768-4773, 2004.
- Boucher Y, Baxter LT and Jain RK: Interstitial pressure gradients in tissue-isolated and subcutaneous tumors: Implications for therapy. *Cancer Res* 50: 4478-4484, 1990.
- Davies CdeL, Lundstrøm LM, Frengen J, Eikenes L, Bruland ØS, Kaalhus O, Hjelstuen MHB and Brekken C: Radiation improves the distribution and uptake of liposomal doxorubicin (Caelyx) in human osteosarcoma xenografts. *Cancer Res* 64: 547-553, 2004.
- Netti PA, Berk DA, Swartz MA, Grodzinsky AJ and Jain RK: Role of extracellular matrix assembly in interstitial transport in solid tumors. *Cancer Res* 60: 2497-503, 2000.
- Davies CdeL, Berk DA, Pluen A and Jain RK: Comparison of IgG diffusion and extracellular matrix composition in rhabdomyosarcomas grown in mice *versus in vitro* as spheroids reveals the role of host stromal cells. *Br J Cancer* 86: 1639-1644, 2002.
- Alexandrakis G, Brown EB, Tong RT, McKee TD, Campbell RB, Boucher Y and Jain RK: Two-photon fluorescence correlation microscopy reveals the two-phase nature of transport in tumors. *Nat Med* 10: 203-207, 2004.
- Erikson A, Tufto I, Bjønnum AB, Bruland ØS and Davies CdeL: The impact of enzymatic degradation on the uptake of differently sized therapeutic molecules. *Anticancer Res* 28: 3557-3566, 2008.
- Eikenes L, Tari M, Tufto I, Bruland ØS and Davies CdeL: Hyaluronidase induces a transcapillary pressure gradient and improves the distribution and uptake of liposomal doxorubicin (Caelyx™) in human osteosarcoma xenografts. *Br J Cancer* 93: 81-88, 2005.
- Periasamy N and Verkman AS: Analysis of fluorophore diffusion by continuous distributions of diffusion coefficients: Application to photobleaching measurements of multicomponent and anomalous diffusion. *Biophys J* 75: 557-657, 1998.
- Feder TJ, BrustMascher I, Slattery JP, Baird B and Webb WW: Constrained diffusion or immobile fraction on cell surfaces: A new interpretation. *Biophys J* 70: 2767-2773, 1996.
- Fodstad Ø, Brøgger A, Bruland Ø, Solheim ØP, Nesland JM and Pihl A: Characteristics of a cell line established from a patient with multiple osteosarcoma, appearing 13 years after treatment for bilateral retinoblastoma. *Int J Cancer* 38: 33-40, 1986.
- Hjelstuen MH, Rasch-Halvorsen K, Brekken C, Bruland Ø and Davies CdeL: Penetration and binding of monoclonal antibody in human osteosarcoma multicell spheroids. *Acta Oncologica* 35: 273-279, 1996.
- Unemori EN and Amento EP: Relaxin modulates synthesis and secretion of procollagenase and collagen by human dermal fibroblasts. *J Biol Chem* 256: 10681-10685, 1990.
- Schnell EA, Eikenes L, Tufto I, Erikson A, Juthajan A, Lindgren M and Davies CdeL: Diffusion measured by fluorescence recovery after photobleaching based on multiphoton excitation laser scanning microscopy. *J Biomed Optics* 13(06): 064037, 2008.
- Brown EB, Wu ES, Zipfel W and Webb WW: Measurement of molecular diffusion in solution by multiphoton fluorescence photobleaching recovery. *Biophys J* 77: 2837-2849, 1999.
- Davies CdeL, Engeseter B, Haug I, Ormeberg IW, Halgunset J and Brekken C: Uptake of IgG in osteosarcoma correlates inversely with interstitial fluid pressure, but not with interstitial constituents. *Br J Cancer* 85: 1968-1977, 2001.
- Woessner JF: The determination of hydroxyproline in tissue and protein samples containing small proportions of this amino acid. *Arch Biochem Biophys* 93: 440-447, 1961.
- Jackson DS and Cleary EG: The determination of collagen and elastin. *In: Methods of Biochemical Analysis*. Glick D (ed.). New York, Interscience Publ., pp. 25-76, 1976.
- Bitter T and Muir HM: A modified uronic acid carbazole reaction. *Anal Biochem* 4: 330-334, 1962.
- Farndale RW, Buttle DJ and Barrett AJ: Improved quantitation and discrimination of sulphated glycosaminoglycans by use of dimethylmethylene blue. *Biochem Biophys Acta* 883: 173-177, 1986.
- Braeckmans K, Peeters L, Sanders NN, De Smedt SC and Demeester J: Three-dimensional fluorescence recovery after photobleaching with the confocal scanning laser microscope. *Biophys J* 85: 2240-2252, 2003.
- Henry CBS and Duling BR: Permeation of the luminal capillary glycocalyx is determined by hyaluronan. *Am J Physiol* 277: H508-H514, 1999.
- Masuda A, Ushida K, Koshino H, Yamashita K and Kluge T: Novel distance dependence of diffusion constants in hyaluronan aqueous solution resulting from its characteristic nano-microstructure. *J Am Chem Soc* 123: 11468-11471, 2001.
- Parameswaran S, Brown LV, Ibbott GS and Lai-Fook SJ: Effect of concentration and hyaluronidase on albumin diffusion across rabbit mesentery. *Microcirculation* 6: 117-126, 1999.
- Qiu XL, Brown LV, Parameswaran S, Marek VW, Ibbott GS and Lai-Fook SJ: Effect of hyaluronidase on albumin diffusion in lung interstitium. *Lung* 177: 273-288, 1999.
- Basu S, Wolgemuth CW and Campagnola PJ: Measurement of normal and anomalous diffusion of dyes within protein structures fabricated *via* multiphoton excited cross-linking. *Biomacromolecules* 5: 2347-2357, 2004.
- Axelrod D, Koppel DE, Schlessinger J, Elson E and Webb WW: Mobility measurement by analysis of fluorescence photobleaching recovery kinetics. *Biophys J* 16: 1055-1069, 1976.

- 28 Brown EB, Mckee T, diTomaso E, Pluen A, Seed B, Boucher Y and Jain RK: Dynamic imaging of collagen and its modulation in tumors *in vivo* using second-harmonic generation. *Nat Med* 9: 796-801, 2003.
- 29 Curran S and Murray GI: Matrix metalloproteinases in tumor invasion and metastasis. *J Pathol* 189: 300-308, 1999.
- 30 Stamenkovic I: Extracellular matrix remodelling: the role of matrix metalloproteinases. *J Pathol* 200: 448-464, 2003.
- 31 Binder C, Hagemann Th, Husen B, Schulz M and Einspanier A: Relaxin enhances *in vitro* invasiveness of breast cancer cell lines by up-regulation of matrix metalloproteases. *Mol Human Reprod* 8: 789-796, 2002.
- 32 Radestock Y, Hoang-Vu C and Hombach-Klonisch S: Relaxin reduces xenograft tumour growth of human MDA-MB-231 breast cancer cells. *Breast Cancer Res* 10: R71, 2008.
- 33 Brekken C, Hjelstuen MH, Bruland ØS and Davies CdeL: Hyaluronidase-induced periodic modulation of the interstitial fluid pressure increases selective antibody uptake in human osteosarcoma xenografts. *Anticancer Res* 20: 3513-3520, 2000.

Received August 28, 2009
Revised December 29, 2009
Accepted January 5, 2010